TITLE:

Photonic bands in two-dimensional microplasma arrays. II. Band gaps observed in millimeter and subterahertz ranges

AUTHOR(S):

Sakaguchi, T; Sakai, O; Tachibana, K

CITATION:

Sakaguchi, T ...[et al]. Photonic bands in two-dimensional microplasma arrays. II. Band gaps observed in millimeter and subterahertz ranges. JOURNAL OF APPLIED PHYSICS 2007, 101(7): 073305.

ISSUE DATE:

2007-04-01

URL:

http://hdl.handle.net/2433/50124

RIGHT:

Copyright 2007 American Institute of Physics. This article may be downloaded for personal use only. Any other use requires prior permission of the author and the American Institute of Physics.

京都大学学術情報リポジトリ
KURENAI
Kyoto University Research Information Repository

京都大学 KYOTO UNIVERSITY
A Self-archived copy in
Kyoto University Research Information Repository
https://repository.kulib.kyoto-u.ac.jp
京都大学学術情報リポジトリ KURENAI 紅 Kyoto University Research Information Repository

JOURNAL OF APPLIED PHYSICS **101**, 073305 (2007)

Photonic bands in two-dimensional microplasma arrays. II. Band gaps observed in millimeter and subterahertz ranges

Takui Sakaguchi, Osamu Sakai,[a] and Kunihide Tachibana
Department of Electronic Science and Engineering, Kyoto University, Kyoto-daigaku Katsura, Nishikyo-ku, Kyoto 615-8510, Japan

(Received 16 September 2006; accepted 22 January 2007; published online 6 April 2007)

Plasma photonic band gaps have been observed in a two-dimensional microplasma array, and we have characterized their properties by both experimental and theoretical results. Microplasma columns ignited in helium near atmospheric pressure formed crystal-like structures in a square lattice with a lattice constant from 1.5 to 2.5 mm. Microwaves in the millimeter range transmitting through the array region attenuated at frequencies of photonic band gap in the Γ-*X* direction, as predicted by the modified plane-wave expansion method. Frequency dependence around the band gap was clarified in the numerical analysis of electromagnetic wave propagation and agreed with experimental results. Electron density in microplasmas was estimated to be 1×10^{13} cm^{-3} from the attenuation rate at the band gap in the Γ-*X* direction. Variation of the lattice constant induced frequency shift of the band gap in the millimeter and subterahertz regions, and so plasma photonic crystal can perform as a dynamically controllable band-stop filter. © *2007 American Institute of Physics*. [DOI: 10.1063/1.2713940]

I. INTRODUCTION

Plasma photonic crystals, which have been investigated in theoretical approaches as one-dimensional[1–3] and two-dimensional[4] functional layers, were extensively explored in the preceding paper from a theoretical point of view.[5] They work as either dielectric or metal photonic crystal systems according to electron plasma frequency. Not only band gaps similar to dielectric photonic crystals but also flat-bands with standing surface waves over wide frequency range, which is unique to plasma photonic crystals, have been verified using two different theoretical methods.[5]

In our recent experimental studies, plasma photonic crystals were found to exhibit unique features such as band gap and abnormal refraction.[6,7] Such studies were stimulated by the recent progress of photonic crystals. In the last decade, photonic crystals formed in dielectric materials have been extensively examined,[8,9] and potential applications have expanded widely in technical fields as well as in scientific interests. Other than ordinary photonic crystals composed of dielectrics, several tunable materials such as liquid crystals have also been investigated to obtain more controllable properties during operations.[10] We selected microplasmas as a tunable material by external control. Plasma production during which dynamical change of refractive index is possible within several microseconds, is one prominent advantage over other tunable materials. Since they have electron density from 10^{12} to 10^{16} cm^{-3}, dielectric constant varies for electromagnetic waves at frequencies from gigahertz to terahertz.

One of our recent experimental studies treated abnormal refraction around electron plasma frequency.[7] We observed enhanced microwave power transmitted through a two-dimensionally periodical microplasma array for a frequency width of a couple of gigahertz in several tens of gigahertz range. There had been some predictions of wave power convergence in periodic dielectric constants such as superlens effects, but we found no exact agreement with our experimental parameters in the previous studies of ordinary photonic crystals.[11,12] We examined equifrequency contours on two-dimensional wave number planes, which indicated that anisotropic energy flows converged into the Γ-*X* direction of the square lattice just above the electron plasma frequency. This observed phenomenon was unique to plasma photonic crystal and has not been reported so far in the periodical structures of other materials.

Another phenomenon verified in our recent experiments was photonic (electromagnetic) band gap due to its refractive index less than 1.[6] In an ordinary photonic crystal composed of dielectrics and vacuum, unidirectional band gap results from dielectric coefficient that has spatial periodicity and takes a relative value (usually more than 2) to vacuum condition. In the case of crystal structure composed of plasmas, dielectric constant is less than 1 and is dependent of electromagnetic wave frequency, where dependence is usually in the Drude model. In cases of plasmas, one can expect two kinds of stop bands: a unidirectional band gap between the adjacent bands and an all-angle stop band at less than the cutoff frequency of the bulk material where wave number becomes zero in the Drude model formula.[13] The width of the unidirectional band gap varies so widely in a plasma photonic crystal, since the ratio of the dielectric constant between plasma and vacuum regions depends on the bulk cutoff frequency. In other words, if we control electron plasma frequency by changing electron density, which is the bulk cutoff frequency in cases of plasmas, band gap width is controllable. This controllability is realized in a plasma photonic crystal but not in photonic crystals composed of dielectrics or metals.[13,14]

[a]Electronic mail: osakai@kuee.kyoto-u.ac.jp

 © 2007 American Institute of Physics

Downloaded 06 Mar 2008 to 130.54.110.22. Redistribution subject to AIP license or copyright; see http://jap.aip.org/jap/copyright.jsp

京都大学 KYOTO UNIVERSITY
A Self-archived copy in
Kyoto University Research Information Repository
https://repository.kulib.kyoto-u.ac.jp
京都大学学術情報リポジトリ KURENAI 紅 Kyoto University Research Information Repository

Our previous experimental results,[6] which were attributed to this unidirectional band gap, showed that wave energy flow along the corresponding direction of the band gap diverges in the vicinity of the band gap frequency. The observed dynamics of millimeter waves near the band gap due to plasma production confirmed a potential controller for wave propagation that has rapid-changing transmittance properties, such as a time-dependent filter. However, signal attenuation along the exact direction of the band gap was unclear. Further experimental investigation has been required to uncover the entire properties of the band gap formed in a plasma photonic crystal. If any defects are present in a lattice of dielectrics, one cannot expect significant signal attenuation at the predicted frequencies. Therefore the observation of clear attenuation at band gap frequency will verify that the periodical structure of dielectric constant is almost perfect without defects. That is, this observation in a plasma photonic crystal is crucial to confirm the quality of periodicity as well as for applications to dynamic band-stop filters.

In this study, we experimentally investigate the photonic band gap formed by microplasma arrays, and its properties are clarified in comparison with theoretical results by a modified plane-wave expansion method and numerical results of electric fields in wave propagation. Around the first band gap in the Γ-*X* direction predicted by the theories, detected transmittance signals through microplasma arrays decrease to less than 20% of its initial level. Variation of lattice constant leads to a shift of band gap frequency, which implies the controllability of stop-band frequency by changing lattice constant in time. Propagation in the vicinity of band gap is investigated numerically by solving wave equations using a finite difference method that enables us to obtain dispersion relation of the infinite array and electric field patterns in a finite array. In Sec. II, the experimental setup for the measurement of millimeter transmittance is described. In Sec. III, experimental results of observed band gaps are shown and parameter dependences are clarified. In Sec. IV, experimental results are examined using numerical results on dispersion relation and wave propagation, followed by a summary in Sec. V.

II. EXPERIMENTAL SETUP

Several electrode configurations have been tested to form two-dimensional microplasma arrays. Specific points in each electrode configuration are described in Sec. III, but the points shared by the configurations are shown below. The homogeneity of the columns throughout the two-dimensional plane is one essential point to remove defect effects against ideal crystal structure. We set a ballast (series) resistor in an individual electrode in the case of dc operation, whereas a dielectric layer with uniform thickness covered metal electrodes in ac operation to maintain constant discharge current over the whole surface. Helium was used as a working gas with significant flow to prevent impurity particles from entering the discharge regions, since too many impurities lower electron density by quenching metastable He atoms.[7] The power supply for the application of discharge voltages synchronously produced both monopolar and bipolar square pulses at a 5 kHz repetition frequency, and they were imposed on the electrodes except for the grounded electrode(s).

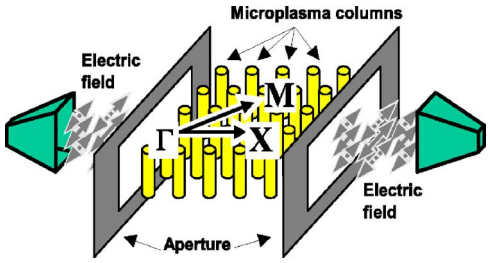

FIG. 1. (Color online) Schematic view of plasma photonic crystal and millimeter setup for detection of wave propagation. Drawn patterns of electric field are in TE mode.

Millimeter waves were transmitted through the microplasma array, as shown in Fig. 1.[6,7] They were launched from a pyramidal horn antenna, where electric fields lie along the shorter axis of the rectangular opening. We arranged TE or TM mode propagation with respect to the two-dimensional array's plane; in TE mode, an electric field is parallel to the array's plane, and in TM mode, it is perpendicular to the plane and parallel to the plasma columns. Another pyramidal horn antenna was set as a detector on the other side of the microplasma array. Each mode was selectively launched since electric fields were tuned in the same direction on both the transmitter and the receiver antenna openings by aligning the angle of the antenna. To guide millimeter waves into the plasma array and prevent waves leaking into the outer region and entering the detector, we placed metal apertures at both the entrance and the exit of the microplasma array region. We confirmed that a metal plate instead of a metal aperture at the exit reduced the detected waves to zero. In the experiments mentioned below, wave propagation in the Γ-*X* direction was investigated, where the direction along the lattice points is Γ-*X* and the diagonal line is Γ-*M*.

III. EXPERIMENTAL RESULTS

A. Band gap observation in a columnar plasma array

Figure 2 shows one electrode configuration for plasma photonic crystals. The configuration of this electrode was an assembly of capillary electrodes proposed by Kundhalt.[15] He used it for uniform atmospheric pressure plasma production, but we set discharge parameters to realize discrete plasma columns. Multiholes through dielectric plates (made of glass epoxy copper clad laminate) determined the lattice constant of the square lattice to be 2.5 mm. The plates were 1.6 mm thick, and the gap between them was 5.0 mm. On one side a metal pin electrode was arranged on each hole and was connected to a ballast (series) resistance (47 kΩ) to assure array uniformity. On the other side a metal plate covered the entire array area, and so the total discharge gap was 8.2 mm long. Bipolar voltage (V_{ac}) pulse was applied on the pin electrode array through the ballast resistors. Alternative discharge current flowed after displacement current to induce charge-up on the surface of the dielectric plate. Although the alternative current level was very low, it supplied initial electrons for main columnar discharge and contributed to the uniformity of the columnar discharge; both ballast resistors and capillary

Downloaded 06 Mar 2008 to 130.54.110.22. Redistribution subject to AIP license or copyright; see http://jap.aip.org/jap/copyright.jsp

京都大学 KYOTO UNIVERSITY
A Self-archived copy in
Kyoto University Research Information Repository
https://repository.kulib.kyoto-u.ac.jp
京都大学学術情報リポジトリ KURENAI 紅 Kyoto University Research Information Repository

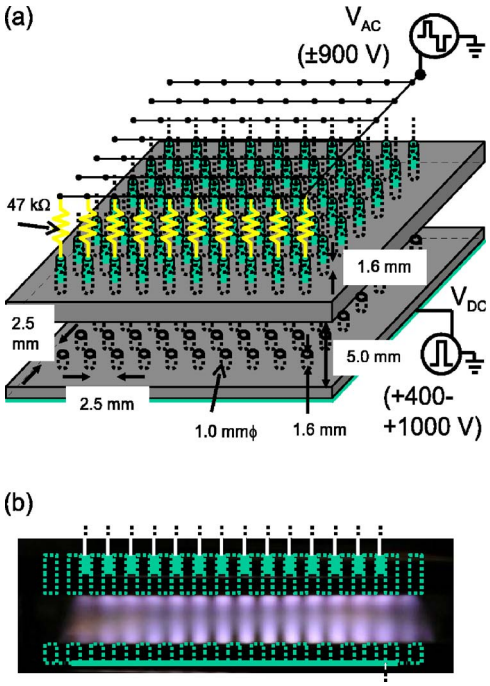

FIG. 2. (Color online) (a) Schematic view of electrode configuration with lattice constant of 2.5 mm. (b) Visible emission pattern of array of microplasma columns in a side view.

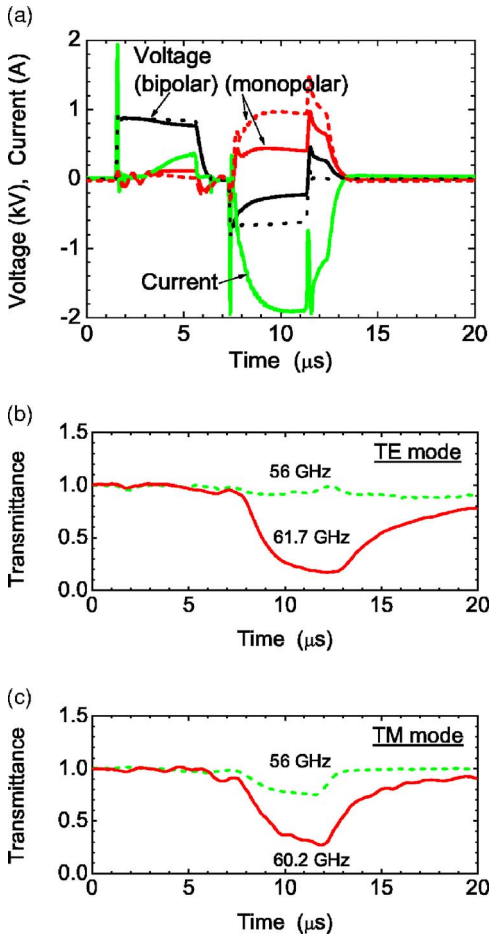

FIG. 3. (Color online) (a) Time evolutions of applied and discharge voltages and discharge currents. Solid and dotted lines in voltage indicate signals at supply output and on electrode, respectively. (b) Transmittance signal of millimeter waves in TE mode. (c) Transmittance signal of millimeter waves in TM mode.

electrode structure played roles in the formation of the uniform columnar microplasma array. After the current was triggered by accumulated charges on dielectrics, the main direct current flowed in a direct current manner. Monopolar voltage pulse (V_{dc}) was imposed on the plate electrode to enhance the main discharges or control their intensity. Discharge gas (He) flowed transversely through the plasma column region at 2.0 l/min. Figure 2(b) illustrates a side view of visible discharge emission, and almost uniform distribution was realized except in one row on the edge.

Figure 3 shows the time evolutions of typical discharge signals and millimeter wave signals in the TE and TM modes. Here the millimeter wave signal is expressed as "transmittance," which is defined as the ratio of the detected signal during discharge and afterglow phases to that before application of the bipolar voltage pulse. The monopolar voltage pulse was superposed in the negative phase of the bipolar pulse, and large discharge current flowed between the metal electrodes. When millimeter wave frequency was less than 60 GHz, almost no change was detected in the transmittance signal. On the other hand, the millimeter waves attenuated to 20% of initial value at 60–63 GHz, where the band gap exists, as predicted in the theory explained in Sec. IV and in the preceding paper.[5] There was not such a large difference of attenuation level of transmittance signals between the TE and TM modes. Signal transition between on and off phases took several 2–3 μs and depends on the concentration of impurity (mainly N_2) in He.[7,16]

Detailed dependences on frequency and discharge current are examined in Fig. 4. First, detailed transmittance signals with fine frequency resolutions verify the reliability of band gap identification. Another important factor is the electron density required to cause enough transmittance drop in the band gap. When we changed the monopolar voltage to see the effects of electron density, observed wave attenuation varied with the amount of the discharge current. Figure 4 shows the frequency dependence of the transmittance at various discharge currents. As seen in Fig. 4(a), discharge current was controlled linearly with monopolar voltage V_{dc}. The plasma had a columnar shape, and so a radial loss of electrons was compensated for through plasma production by an electric field along the column axis. This electric field was mainly supported by monopolar pulse, and consequently, electron density was raised as monopolar voltage increased. Simultaneously the attenuation level of transmittance changed with discharge current, which verified the change of electron density and corresponding dielectric constant. Figure 4(b) demonstrates that wave attenuation became larger as discharge current increased, which is attributed to the enhancement of electron density and the consequent change of the dielectric constant. The specific value of electron density will be estimated in Sec. IV. As far as frequency dependence is concerned, when we set the frequency higher than 63 GHz, which is more than the band gap frequency, there was still wave attenuation to a certain extent. This attenuation will be discussed again in Sec. IV.

Downloaded 06 Mar 2008 to 130.54.110.22. Redistribution subject to AIP license or copyright; see http://jap.aip.org/jap/copyright.jsp

京都大学 KYOTO UNIVERSITY
A Self-archived copy in
Kyoto University Research Information Repository
https://repository.kulib.kyoto-u.ac.jp
京都大学学術情報リポジトリ KURENAI 紅 Kyoto University Research Information Repository

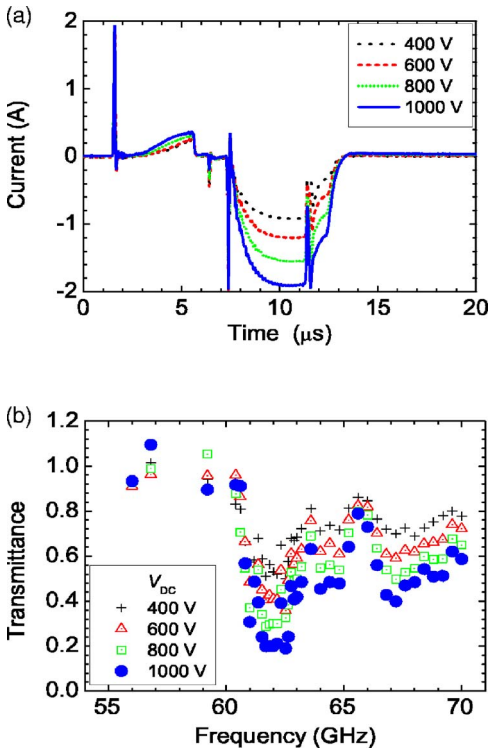

FIG. 4. (Color online) (a) Time evolutions of discharge currents for various applied monopolar voltage V_{dc}. (b) Frequency dependence of transmittance signals of millimeter waves in TE mode as a function of V_{dc}. Discharge gas was He at 200 Torr, $V_{ac}=900V_{0p}$, and the row number of plasma columns is 30.

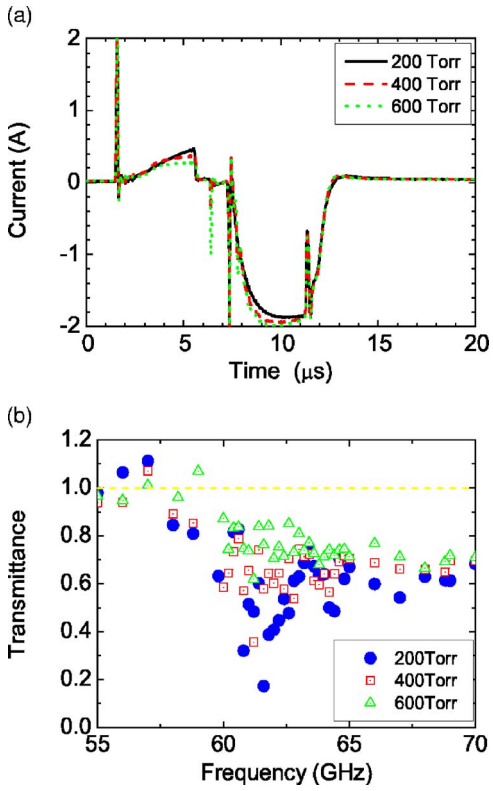

FIG. 5. (Color online) (a) Time evolutions of discharge currents for various He gas pressure. (b) Frequency dependence of transmittance signals of millimeter waves in TE mode as a function of gas pressure. $V_{ac}=900V_{0p}$, $V_{dc}=1000V_{0p}$, and the row number of plasma columns is 30.

Gas pressure is another important factor for dielectric constant ε, since it is expressed using electron elastic collision frequency ν_m as

$$\varepsilon = 1 - \left(\frac{\omega_{pe}}{\omega}\right)^2 \frac{1}{1 - j(\nu_m/\omega)}, \tag{1}$$

and the real part of ε will be derived as

$$\mathrm{Re}(\varepsilon) = 1 - \frac{{\omega_{pe}}^2}{\omega^2 + {\nu_m}^2}. \tag{2}$$

When gas pressure is raised and dielectric constant is reduced, the band gap becomes narrower and more difficult to be detected. Figure 5(b) shows the frequency dependence of transmittance signal at various gas pressures. Note that discharge current was set to be constant through the pressure range by changing the monopolar voltage, as shown in Fig. 5(a). At 200 Torr, clear transmittance drop was observed between 60 and 63 GHz, but such drop became smaller as the pressure was increased. This fact was consistent with the predicted change of dielectric constant shown in Eqs. (1) and (2).

Band gap is usually defined in an infinite periodicity of dielectric constant, but it is impossible to realize such an exact condition in experiments. Here we examined the effects of the finite size of the microplasma arrays in Fig. 6. In comparison with the case of 30 rows, wave attenuation was smaller in the case of 17 rows. Due to a lower ratio of dielectric constant between plasma and vacuum regions, plasma photonic crystals require more rows than cases of an ordinary photonic crystal.[17] However, other advantages, such as controllability in space and rapid change in time, intensify the functionality of plasma photonic crystals. The number of rows required for wave attenuation will be discussed in Sec. IV.

B. Dependence of band gap frequency on lattice constant

Another electrode configuration was used to develop plasma photonic crystals of smaller lattice constant. Figure 7(a) displays electrode structure with visible discharge emission from plasma photonic crystals with a lattice constant of

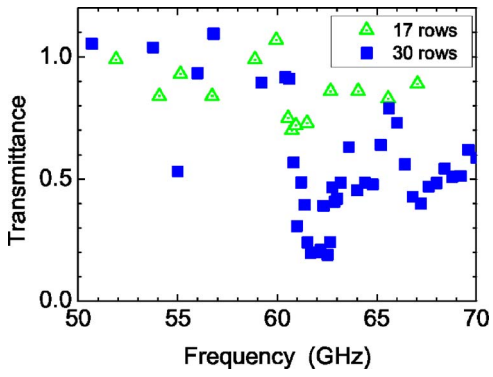

FIG. 6. (Color online) Frequency dependence of transmittance signals of millimeter waves in TE mode as a function of row numbers of plasma columns along wave propagation. Discharge gas was He at 200 Torr, $V_{ac}=900V_{0p}$, and $V_{dc}=1000V_{0p}$.

Downloaded 06 Mar 2008 to 130.54.110.22. Redistribution subject to AIP license or copyright; see http://jap.aip.org/jap/copyright.jsp

京都大学 KYOTO UNIVERSITY
A Self-archived copy in
Kyoto University Research Information Repository
https://repository.kulib.kyoto-u.ac.jp
京都大学学術情報リポジトリ KURENAI 紅 Kyoto University Research Information Repository

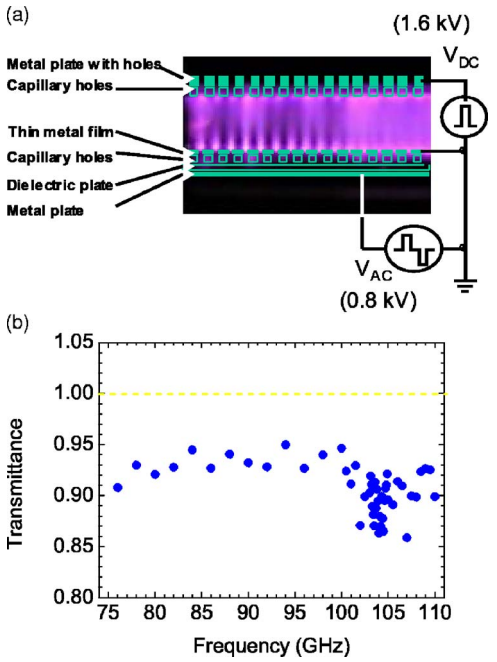

FIG. 7. (Color online) (a) Schematic view of electrode configuration with lattice constant of 1.5 mm and visible emission pattern of array of microplasma columns in a side view. (b) Frequency dependence of transmittance signals of millimeter waves in TE mode. Discharge gas was He at 200 Torr, $V_{ac}=900V_{0p}$, $V_{dc}=1000V_{0p}$, and the row number of plasma columns is 33.

1.5 mm. The upper electrode was a multicapillary type that resembles the one in Fig. 2, and the lower electrode consists of a multicapillary type covered with thin metal film with aligned holes, similar to the one shown by Sakurai *et al.*[18] The inserted insulator film functioned as a dielectric barrier to make the plasma columns uniform over the array. The lower electrode served as a cathode electrode with electron supplier generated by microdischarges between the metal plate and the metal thin film. Visible emission verified the function of the electron supplier since emission intensity was higher on the lower electrode side. The resultant array size is 33×33 lattices, where 33 rows of a microplasma column with a diameter of 0.6 mm were along the Γ-X direction.

Figure 7(b) exhibits frequency dependence of transmittance in the configuration shown in Fig. 7(a), where detected propagation was set to be along the Γ-X direction. Although the attenuation rate was smaller than as in Fig. 4, a similar tendency was observed: the transmittance signal showed a clear drop at 102–106 GHz. The smaller attenuation rate might reflect the low ratio of dielectric constant in the plasma and vacuum regions, since the frequency was relatively high in comparison with potential electron plasma frequency. Inhomogeneity of the plasma array observed in Fig. 7(a) might work as lattice defects, and it would also make the band gap properties ambiguous.

The other electrode configuration for a lattice constant of 2.1 mm was shown in our previous report.[6,7] In brief, the electrode set consisted of a coaxial hollow dielectric barrier type[19] and a plane flat metal plate. We also produced periodical plasma array in square lattice using this configuration and observed change of energy flow from the Γ-X to the Γ-M direction with small signal attenuation in the Γ-X direction. Unclear signal attenuation might be due to the finite size of the array and possible lattice defects. The change of wave energy flow near the band gap will be discussed in Sec. IV. All the results from the different electrode sets about the first band gap in the Γ-X direction were summarized in Fig. 8, where the inset line indicates the approximate band gap condition at which $\omega a/2\pi c=0.5$. Since all experimental data points were along this theoretical line, we could clarify the identification of this band gap between the first and the second bands in the Γ-X direction.

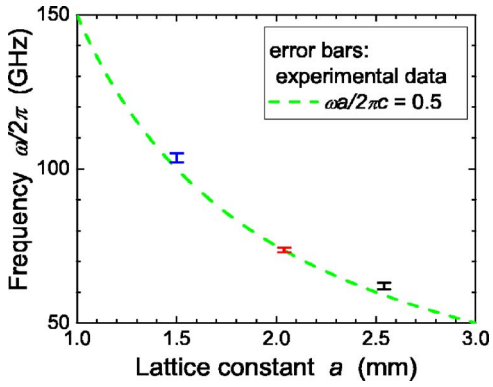

FIG. 8. (Color online) Band gap frequency as a function of lattice constant.

IV. DISCUSSION

To analyze the band diagram and wave propagation quantitatively, we have developed two methods so far that were demonstrated in their primitive level[6,7] and described in greater details with more precise approximation in a preceding paper.[5] Briefly, we developed a modified plane-wave expansion method for dielectric constant in plasmas, where dielectric constant is a function of frequency in the Drude model. We also included the effects of elastic collision frequency, which is comparable to wave frequency in our experimental parameters. Another technique to derive band diagrams is based on the finite difference method (FDM), where the periodical (Bloch theorem) boundary condition was adapted and arbitrary spatial distribution of dielectric constant can be treated.

The first band gap, which is the main focus of this experimental study, was formed between the first and the second bands in the Γ-X direction. Figure 9 shows detailed band structure in two-dimensional plasma photonic crystal with $n_e=10^{13}$ cm^{-3} near the first band gap in the Γ-X direction, derived by a FDM-based technique in two-dimensional wave number plane (k_x,k_y). Here, cases with $k_y=0$ show propagation in the Γ-X direction, and those with $k_x=k_y$ represent propagation in the Γ-M direction. Electron density in collisionless microplasmas is assumed to be distributed in a slab shape. The band gap, which exists at 60–63 GHz in the Γ-X direction, extends to the band gap in the Γ-M direction with its frequency upshifted. On the whole, equifrequency contours in the bottom plot show concentric structure, indicating that wave propagation is isotropic. The outstanding point emerging in this figure is the deformation of equifrequency plots near the X point. The interval of the contours widens, and energy flow approximately proportional to group veloc-

Downloaded 06 Mar 2008 to 130.54.110.22. Redistribution subject to AIP license or copyright; see http://jap.aip.org/jap/copyright.jsp

京都大学 KYOTO UNIVERSITY
A Self-archived copy in
Kyoto University Research Information Repository
https://repository.kulib.kyoto-u.ac.jp
京都大学学術情報リポジトリ KURENAI 紅 Kyoto University Research Information Repository

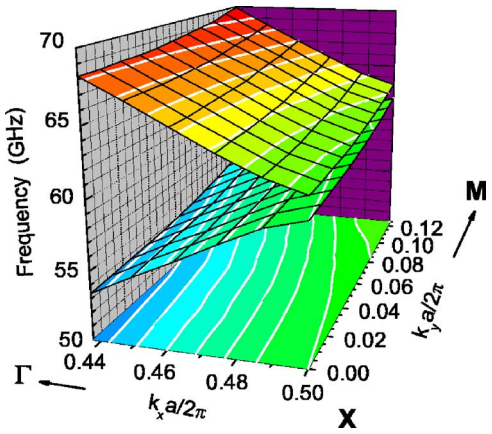

FIG. 9. (Color online) Detailed dispersion around X point drawn in two-dimensional wave number plane. Collisionless plasma column has a diameter of 1.0 mm in a square lattice with lattice constant of 2.5 mm and the electron density was 10^{13} cm^{-3}.

ity ($d\omega/dk$) becomes convex and is not parallel to phase velocity (ω/k). That is, the wave energy cannot be delivered in the Γ-X direction *at* this band gap and, furthermore, the energy flow carried by the wave propagating in the Γ-X direction diverges to the Γ-M direction *near* the band gap frequency. The latter feature was in the experimental results in our previous report.[6] These two factors decrease the wave energy at and near the band gap in the Γ-X direction.

Another unsolved factor observed in the experiments was abnormal wave attenuation beyond band gap frequency. These phenomena are investigated here using the FDM-based technique in the scheme of "supercell."[20] Note that electric fields are solved on the two-dimensional propagation plane, so the TE mode is assumed in the calculation. As shown in Fig. 10(b), we set ten sequential lattices in the Γ-X direction, and the wave is excited from the left and absorbed on the right side where two different resistance layers are set to absorb the transmitted power and to minimize reflection from the wall. The periodical boundary condition of the Bloch theorem is adapted in the perpendicular direction of the long lattice array. Figures 10(a) and 10(b) show the numerical results of electric field out of phase with the current source in Γ-X propagation in which k_y=0, where electric field profiles calculated in the adjacent three supercells are repeated. In cases without plasmas in Fig. 10(a), no wave attenuation is observed throughout the target frequencies. Just below the band gap frequency in cases with plasmas (57.5 GHz) in Fig. 10(b), wave attenuation is not so large, but large attenuation is observed at the midpoint of the band gap (61.5 GHz). Significant attenuation continues even when the frequency is raised from the band gap region (e.g., 65.5 GHz), which is consistent with experimental observations.

This wave damping along the propagation direction in the band gap condition is enhanced as electron density or the number of plasma columns along the propagation direction increases. Using the same technique in Fig. 10, the transmittance of propagating waves is derived. Figure 11 shows wave transmittance as a function of electron density in two cases corresponding to experimental array size. We assume that

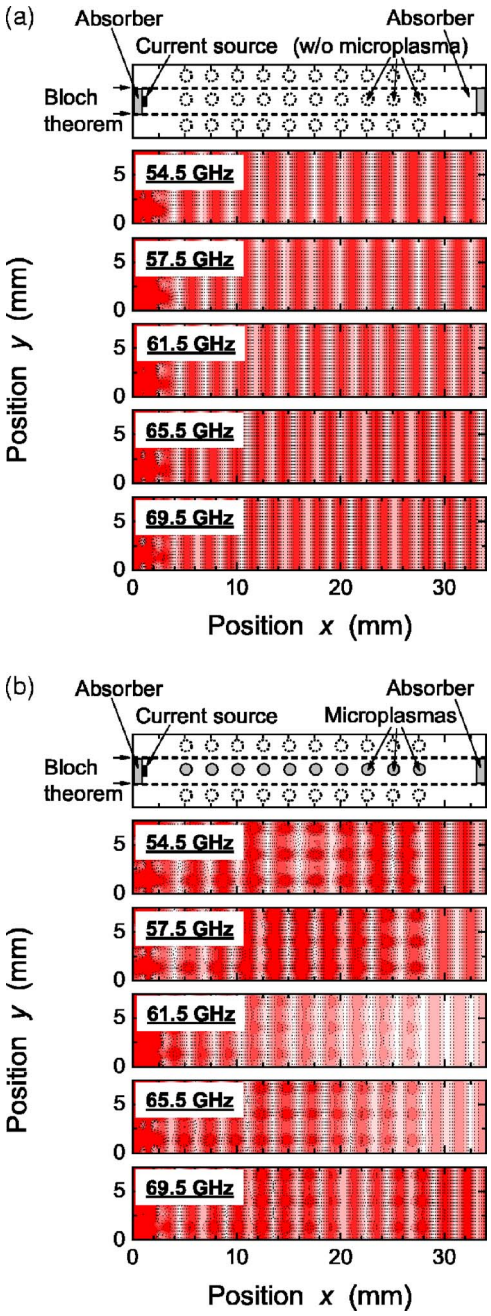

FIG. 10. (Color online) (a) Numerical results of electric fields in supercell method without plasmas. Calculated data are repeated laterally to show continuity between supercells. Calculation geometry of arrangement of two-dimensional plasma column for "supercell" method by FDM is also shown. (b) Numerical results of electric fields in supercell method with collisionless plasmas with electron density of 2×10^{13} cm^{-3}.

absorption in a microplasma array is negligible since experimental data show almost no damping of waves below the first band gap (about 60–63 GHz at a=2.5 mm). Transmittance T is calculated on the assumptions that wave power transmitting the array region is all absorbed by resistance layers, and that reflected waves from the array region, estimated by reflectance R with $T+R=1$, are superposed on the initial wave power ($T+R$) in front of the array region, where wave power is proportional to the square of electric fields integrated over the corresponding half-wavelength area. Figure 11 shows that electron density more than 2×10^{13} cm^{-3}

Downloaded 06 Mar 2008 to 130.54.110.22. Redistribution subject to AIP license or copyright; see http://jap.aip.org/jap/copyright.jsp

京都大学 KYOTO UNIVERSITY
A Self-archived copy in
Kyoto University Research Information Repository
https://repository.kulib.kyoto-u.ac.jp
京都大学学術情報リポジトリ KURENAI 紅 Kyoto University Research Information Repository

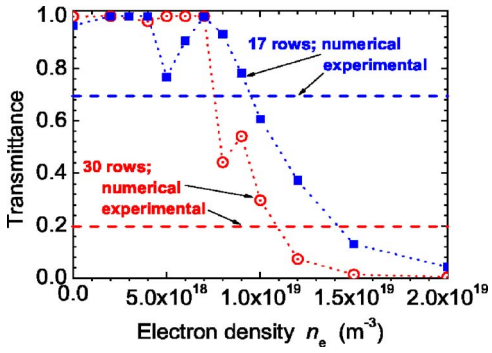

FIG. 11. (Color online) (a) Numerical results of transmittance as a function of electron density and column rows calculated using "supercell" method by FDM. Inset: horizontal lines are experimental results displayed in Fig. 6.

nearly prohibits waves in this band gap from propagating in the Γ-*X* direction. That is, this figure indicates future paths for further reduction of wave transmittance by changing electron density and plasma row number along the propagation. The observed transmittance at the band gap in the experiments was around 20% of its initial value at maximum and more wave attenuation would be required for a complete band-stop filter. For this purpose, either way will work well; the first method is increase of electron density, and the second is increasing column row number. For instance, from Fig. 11, transmittance at 30 rows is 0.3% (−25 dB) of its initial value when electron density is 2×10^{13} cm^{-3}.

The numerical results shown in Fig. 11 also indicate that electron density in microplasmas forming a two-dimensional array in the above experiments is estimated to be about 1×10^{13} cm^{-3} to fit the experimental data shown in Fig. 6. This derived value (1×10^{13} cm^{-3}) is in good agreement with the electron density assumed in the theoretical calculations, as exhibited in Fig. 9 in this paper and the figures in the preceding paper.[5]

These experimental and theoretical results clarified the property of unidirectional band gap in plasma photonic crystals. The dependence on frequency was somewhat similar to photonic crystal composed of dielectric rods.[17] The periodicity of dielectric constant resulting from the dispersion of plasmas expressed in Eq. (1) formed this band gap. The most important difference from ordinary photonic crystal is that a plasma photonic crystal has a dynamic feature about its presence, as clearly shown in Fig. 3. This feature will change the lattice pattern by driving individual plasma columns externally, and so its stop-band function can be controlled each time for a specific purpose. For instance, when we add an electric switch in series to each metal pin electrode in the configuration in Fig. 2, we can control a plasma pattern by active-matrix driving: if plasmas are created in every other row and column, the lattice constant will be doubled and the band gap will emerge around 30 GHz. That is, this microplasma array works as a dynamic (rapidly tunable) band-stop filter. Unfortunately, this frequency (30 GHz) is out of range in our present experimental setup. In other senses, although this band gap is not all angle but unidirectional, it will work as an energy flow converter (i.e., from Γ-*X* to Γ-*M*). The other feature of plasma photonic crystal is that it depends on electron elastic collision, and sometimes this feature deteriorates its stop-band function. Further increase of electron density will expand its working frequency to terahertz waves, where functional wave controllers have not been accomplished in solid-state devices.

V. CONCLUSION

We investigated the band gap properties of electromagnetic waves propagating in one direction of plasma photonic crystals. A millimeter wave at 33–110 GHz in TE or TM mode was injected into a two-dimensional plasma column array, and transmittance signal through the array was detected. At frequencies of band gap in the Γ-*X* direction predicted theoretically, large signal attenuation less than 20% was observed. Such properties of the detected signals were consistent with theoretical results based on modified plane-wave expansion and finite difference methods. Comparisons of experimental data with theoretical results also led to estimation of electron density in microplasmas around 1×10^{13} cm^{-3}. Band gap frequency could be varied by changing the lattice constant, leading to a function of dynamic and time-controllable band-stop filter in millimeter and subterahertz regions.

ACKNOWLEDGMENTS

This work was supported by a Grant-in-Aid for Scientific Research from the Japanese Ministry of Education, Culture, Sports, Science and Technology and by the project to develop "innovative seeds" from the Japan Science and Technology Agency.

[1] J. Faith, S. P. Kuo, and J. Huang, Phys. Rev. E **55**, 1843 (1997).
[2] D. K. Kalluri, *Electromagnetics of Complex Media* (CRC Press, Boca Raton, 1998).
[3] H. Hojo and A. Mase, J. Plasma Fusion Res. **80**, 89 (2004).
[4] H. Hojo, N. Uchida, and A. Mase, Plasma Fusion Res. **1**, 21 (2006).
[5] O. Sakai, T. Sakaguchi, and K. Tachibana, J. Appl. Phys. **101**, 073304 (2006), preceding paper.
[6] O. Sakai, T. Sakaguchi, and K. Tachibana, Appl. Phys. Lett. **87**, 241505 (2005).
[7] O. Sakai, T. Sakaguchi, Y. Ito, and K. Tachibana, Plasma Phys. Controlled Fusion **47**, B617 (2005).
[8] E. Yablonovitch, Science **289**, 557 (2000).
[9] *Roadmap on Photonic Crystals*, edited by S. Noda and T. Baba (Kluwer Academic, Boston, 2003).
[10] S. W. Leonard *et al.*, Phys. Rev. B **61**, R2389 (2000).
[11] M. Notomi, Phys. Rev. B **62**, 10696 (2000).
[12] C. Luo, S. G. Johnson, J. D. Joannopoulos, and J. B. Pendry, Phys. Rev. B **65**, 201104 (2002).
[13] K. Sakoda, N. Kawai, T. Ito, A. Chutinan, S. Noda, T. Mitsuyu, and K. Hirano, Phys. Rev. B **64**, 045116 (2001).
[14] V. Kuzmiak and A. A. Maradudin, Phys. Rev. B **55**, 7427 (1997).
[15] E. E. Kunhaldt, IEEE Trans. Plasma Sci. **28**, 189 (2000).
[16] K. Tachibana, Y. Kishimoto, and O. Sakai, J. Appl. Phys. **97**, 123301 (2005).
[17] W. M. Robertson, G. Arjavalingam, R. D. Maede, K. D. Brommer, A. M. Rappe, and J. D. Joannopoulos, Phys. Rev. Lett. **30**, 2023 (1992).
[18] T. Sakurai, S. Yoshida, H. Yoshikawa, S. Yoshizawa, and A. Morimitsu, Jpn. J. Appl. Phys., Part 1 **44**, 1441 (2005).
[19] O. Sakai, Y. Kishimoto, and K. Tachibana, J. Phys. D **38**, 431 (2005).
[20] M. L. Povinelli, S. G. Johnson, S. Fan, and J. D. Joannopoulos, Phys. Rev. B **65**, 075313 (1992).

Downloaded 06 Mar 2008 to 130.54.110.22. Redistribution subject to AIP license or copyright; see http://jap.aip.org/jap/copyright.jsp